Prediction and Planning Methods of Bipedal Dynamic Locomotion Over Very Rough Terrains

Luis Sentis, Benito Fernandez, and Mike Slovich

Abstract

Although the problem of dynamic locomotion in very rough terrain is critical to the advancement of various areas in robotics and health devices, little progress has been made on generalizing gait behavior with arbitrary paths. Here, we report that perturbation theory, a set of approximation schemes that has roots in celestial mechanics and non-linear dynamical systems, can be adapted to predict the behavior of non closed-form integrable state-space trajectories of a robot's center of mass, given its arbitrary contact state and center of mass (CoM) geometric path. Given an arbitrary geometric path of the CoM and known step locations, we use perturbation theory to determine phase curves of CoM behavior. We determine step transitions as the points of intersection between adjacent phase curves. To discover intersection points, we fit polynomials to the phase curves of neighboring steps and solve their differential roots. The resulting multi-step phase diagram is the locomotion plan suited to drive the behavior of a robot or device maneuvering in the rough terrain. We provide two main contributions to legged locomotion: (1) predicting CoM state-space behavior for arbitrary paths by means of numerical integration, and (2) finding step transitions by locating common intersection points between neighboring phase curves. Because these points are continuous in phase they correspond to the desired contact switching policy. We validate our results on a human-size avatar navigating in a very rough environment and compare its behavior to a human subject maneuvering through the same terrain.

1 State of the Art

In dynamic walking we can classify techniques in various categories: (1) trajectory-based techniques, (2) limit cycle-based techniques, (3) prediction of contact, and (4) hybrids of the previous three.

All of the authors are with the University of Texas at Austin
e-mails: lsentis@austin.utexas.edu, {benito}{slovich}@mail.utexas.edu

Trajectory-based techniques are techniques that track a time-based joint or task space trajectory according to some locomotion model such as the *Zero Moment Point* (ZMP). The state of the art of these methods includes generalized multi-contact locomotion behaviors, developed in [1] and more recenlty, a time delay extension to the ZMP method for locomotin in moderately uneven terrain, developed by [2].

Prediction of contact placement are techniques that use dynamics to estimate suitable contact transitions to produce locomotion or regain balance. In [3], simple dynamic models are used to predict the placement of next contacts to achieve desire gait patterns. Finding feasible CoM static placements given frictional constraints was tackled in [4, 5]. In [6], *stable locomotion*, in the wide sense of not falling down, is studied by providing velocity based stability margins. This work is used to regain stability when the robot's is pushed out, and lead to the concept of Capture Point.

Limit cycle based techniques were pioneered by McGeer [7] through the field of *passive dynamic walking*. In [8] the authors study orbital stability, and the effect of feedback control to achieve asymptotic stability. Optimization of open-loop stability is investigated in [9]. In [10], the authors analyze the energetic cost of bipedal walking and running as well as the role of leg sequencing. In [11], the authors developed a dynamic walker using artificial muscles and principles of stability of passive walkers. In [12], a methodology for the analysis of state-space behavior and feedback control are presented for various physical robots. *Step recovery* in response to perturbations is studied in [13] supported by a linear bipedal model in combination with an orbital energy controller. In [14], the selection of gait patterns based on studying the interplay between robustness against perturbations and leg compliance is investigated.

Hybrid methods include [15], where the stability of passive walkers is studied and a controller obeying the rule, "in order to prevent falling backward the next step, the swing leg shouldn't be too far in front", in the words of the author, is suggested. Stochastic models of stability and its application for walking on moderately rough unmodeled terrain are studied in [16]. The design of non-periodic locomotion for uneven terrain is investigated in [17]. In [18], the authors explore the design of pasitivity-based controllers to achieve walking on different ground slopes. Optimization-based techniques for locomotion in rough terrains are presented in [19]. Locomotion in very rough terrain is presented in [20], where the authors exploit optimization and static models as a means to plan locomotion. More recently, the authors of [21] have proposed a very efficient planner that can generate a discrete sequence of multi-contact stances using static criteria. Also recently, we made a theoretical contribution in the form of an extended abstract [22] to enable walking at fast speeds in very difficult variable terrain.

Hybrid methods: In [15], the stability of passive walkers is studied and a controller obeying the rule, "in order to prevent falling backward the next step, the swing leg shouldn't be too far in front", in the words of the author,

is suggested. Stochastic models of stability and its application for walking on moderately rough unmodeled terrain are studied in [16]. The design of non-periodic locomotion for uneven terrain is investigated in [17]. In [18], the authors explore the design of passivity-based controllers to achieve walking on different ground slopes. Optimization-based techniques for locomotion in rough terrains are presented in [19]. One of the most impressive works in locomotion in very rough terrain is presented in [20], where the authors exploit optimization as a means to plan locomotion. However, the planner is derived from static models of balance.

2 Summary of our approach

We present here a new contribution that tackles rough terrain locomotion by exploring *CoM state-space manifolds* and *transitional contact states.*

Our approach, can be explained algorithmically in terms of various phases, namely (1) geometric planning, (2) perturbation-based CoM phase generation, and (3) dynamic step planning based on locating common intersection points between neighboring CoM phase curves. The geometric planning phase consists of applying standard kinematic planning techniques to obtain initial guesses of feet contact locations and CoM geometric path. Perturbation-based CoM phase generation is our first contribution and consists on: (1) formulating CoM accelerations based on the contact state, (2) incorporating the dependencies between Sagittal and vertical accelerations due to the given CoM geometric path, and (3) using perturbation theory to predict phase curves of the CoM in the vicinity of the step contacts and given initial and final conditions of the step. The step solver is our second contribution and consists on finding step transitions by locating common intersection points between neighboring CoM phase curves. Because these points are continuous in phase they correspond to the desired contact switching policy.

3 Mathematic derivations

3.1 Dynamic behavior from single contact point

Dynamic equilibrium (a principle derived from Newton's Laws of Motion and Lagrange-d'Alembert Formalism) states that the sum of acting moments on a moving system equals the net inertial moment. Given a contact scenario, such as the one shown in Figure 1, this principle translates into the following moment balance expression
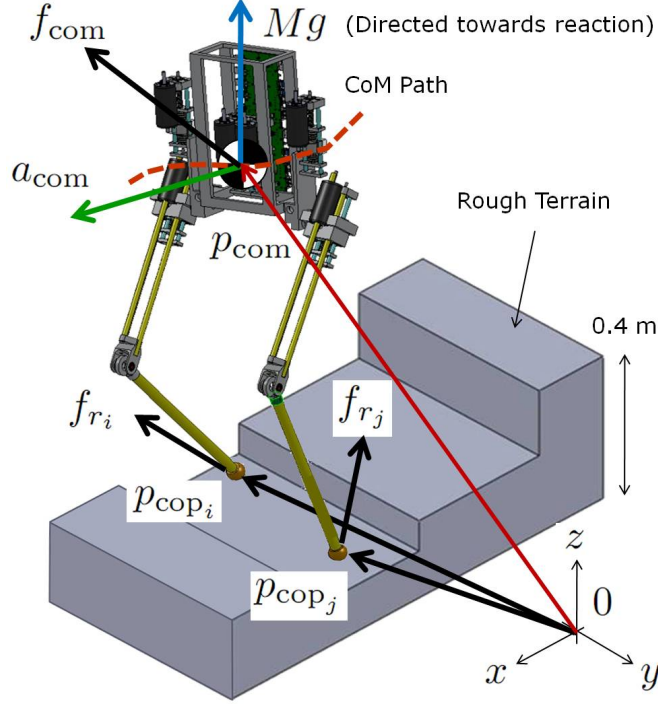
Fig. 1 Definition of coordinates of center of mass (CoM), center of pressures (CoP), and their position coordinates, p_{com}, p_{cop_i}, p_{cop_j}. Also shown are reaction forces, f_{r_i}, f_{r_j} and the CoM's acceleration, a_{com}.

$$\sum_{i=1}^{n_s} p_{\mathrm{cop}_i} \times f_{r_i} + \sum_{i=1}^{n_s} m_{r_i} = p_{\mathrm{com}} \times \left(f_{\mathrm{com}} + M\,g \right) + m_{\mathrm{com}}, \qquad (1)$$

where p_{cop_i} is the i-th foot contact pressure point (with respect to the co-ordinate origin), $i = 1, \ldots, n_s$, the number of supporting limbs; f_{r_i} and m_{r_i} are the reaction force and moment at the pressure point; p_{com} is the vector from the origin (of coordinates) to the CoM; f_{com} and m_{com} are the net force and moment acting on the CoM; M is the robot's mass and g is gravitational constant expressed upwards in the direction of the reaction forces.

Due to the complexity of the algorithms, in this paper we will first address locomotion as transitions involving one support limb. Therefore, the above equation becomes

$$p_{\mathrm{cop}_k} \times f_{r_k} + m_{r_k} = p_{\mathrm{com}} \times \left(f_{\mathrm{com}} + M\,g \right) + m_{\mathrm{com}}, \qquad (2)$$

where, k is the limb in contact with the terrain, p_{cop_k} is the limb's Center of Pressure (CoP) point. The above equation is vectorial and represents three

orthogonal moments. Because we aim first at controlling planar robots in the Sagittal direction, we consider only solutions that produce accelerations in that direction, i.e.

$$\left[p_{\mathrm{cop}_k} \times f_{r_k} = p_{\mathrm{com}} \times (f_{\mathrm{com}} + M\,g) + m_{\mathrm{com}} \right]^{\mathcal{Y}}. \tag{3}$$

where the $\mathcal{Y}$ symbolizes the Sagittal plane (x-coordinate for frontal direction and z-coordinate for vertical).

Considering dynamic equilibrium in forces we obtain

$$f_{r_k} = f_{\mathrm{com}} + M\,g, \tag{4}$$

and therefore we can rearrange Equation (3) as

$$\left[\left(p_{\mathrm{com}} - p_{\mathrm{cop}_k} \right) \times f_{rk} \right]^{\mathcal{Y}} = m_{\mathrm{com}}^{\mathcal{Y}}. \tag{5}$$

Solving this equation for the CoP in the Sagittal direction leads to the solution

$$p_{\mathrm{cop}_k[x]} = p_{\mathrm{com}[x]} - \frac{f_{r_{[kx]}}}{f_{r_{[kz]}}} \left(p_{\mathrm{com}[z]} - p_{\mathrm{cop}_k[z]} \right) - \frac{m_{\mathrm{com}[y]}}{f_{r[kz]}}. \tag{6}$$

Considering that $f_{r_{[kx]}} = Ma_{\mathrm{com}[x]}$, and $f_{r_{[kz]}} = M(a_{\mathrm{com}[z]} + g)$ we rewrite the above equation as

$$a_{\mathrm{com}[x]} = \frac{\left(p_{\mathrm{com}[x]} - p_{\mathrm{cop}_k[x]} \right)\left(a_{\mathrm{com}[z]} + g \right)}{p_{\mathrm{com}[z]} - p_{\mathrm{cop}_k[z]}} \tag{7}$$

Here, we have assumed a point mass model of the robot, with all of its weight located at its center of mass. As such, there are no inertial moments generated about the center of mass. Also, note that a similar equation could be derived for accelerations in the lateral direction, but for the sake of simplicity we do not consider them in this first study.

3.2 Integration of geometric path

Considering that $a_{\mathrm{com}[x]} \triangleq \ddot{p}_{\mathrm{com}[x]}$, the above equation is dynamic and non-linear. As such, the major challenge that it poses is that it does not have a closed form solution, specially if $p_{\mathrm{com}[z]}$ and $a_{\mathrm{com}[z]}$ are time varying. This difficulty corresponds to the case of our study.

Almost all previous work that has addressed Equation (7) has tackled the solution by simplifying it, constraining CoM trajectories to a fixed height, i.e. $p_{\mathrm{com}[z]} = \mathrm{constant}$. These type of solutions have led to the concept of the Zero Moment Point (ZMP). However, in doing so, locomotion trajectories cannot

Kinematic Path is Downward Line

Kinematic Path is Sine Curve
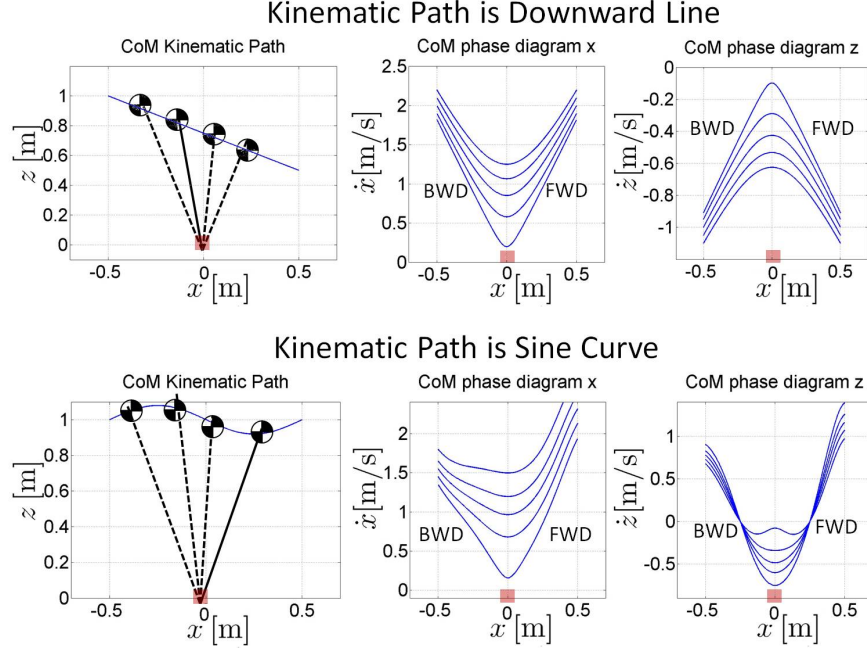
Fig. 2 Phase diagrams of CoM behavior using perturbation theory: These phase diagrams correspond to Matlab simulations of CoM behavior given a foot contact point, a desired CoM kinematic path, and varying boundary conditions given at the apex of the step (i.e. when the CoM is directly above the foot contact point).

be considered for arbitrary terrains nor natural motion involving vertical changes of the hip can be predicted. Therefore, our first contribution is on predicting the behavior corresponding to the general case of Equation (7). Because there are two variables that need to be solved, i.e. the trajectories of the center of mass on the Sagittal and vertical directions, we need to first seed geometric dependencies based on an initial guess. There are many options to determined these dependencies, ranging from ensuring kinematic constraints, generating biomimetic patterns, or minimizing electric and mechanical power. For the time being, let us pick the option of ensuring kinematic constraints.

In such case, one simple dependency that fulfills the needs is to draw a piecewise linear geometric path of the humanoid's CoM behavior that changes slope with the terrain while complying with kinematic constraints. In Figure 2 we depict two hypothetical paths, one linear and one sinusoidal. Let us consider the linear case first with a static contact and use it to predict the CoM dynamic behavior. More generally, if the CoM geometric path is piecewise linear, it can be specified through equations of two or more intersecting lines, i.e.

$$p_{\text{com}[z]} = \begin{cases} a_1 \, p_{\text{com}[x]} + b_1, & p_{\text{com}} \in \mathbb{P}_1 \\[2mm] a_2 \, p_{\text{com}[x]} + b_2, & p_{\text{com}} \in \mathbb{P}_2 \\[2mm] \quad\vdots \\[2mm] a_N \, p_{\text{com}[x]} + b_N, & p_{\text{com}} \in \mathbb{P}_N \end{cases} \qquad (8)$$

where, $\mathbb{P}_k$ represents the path of the CoM over step k, a_i represents the slope of the piecewise lines, and b_i represents the corresponding vertical crossing points. Moreover, the acceleration profile can be extracted by differentiating twice the above piecewise equation, i.e.

$$p_{\text{com}[z]} = a_i \, p_{\text{com}[x]} + b_i \; \Rightarrow \; a_{\text{com}[z]} = a_i \, a_{\text{com}[x]}. \qquad (9)$$

Plugging the above acceleration in (7) we get

$$a_{\text{com}[x]} = \frac{\left(p_{\text{com}[x]} - p_{\text{cop}_k[x]}\right)\left(a_i \, a_{\text{com}[x]} + g\right)}{a_i \, p_{\text{com}[x]} + b_i - p_{\text{cop}_k[z]}}, \qquad (10)$$

and since $a_{\text{com}[x]}$ appears both on the left and right hand sides, we can rewrite the equation as

$$a_{\text{com}[x]} = \frac{\left(p_{\text{com}[x]} - p_{\text{cop}_k[x]}\right) \cdot g}{\left(b_i + a_i \, p_{\text{cop}_k[x]} - p_{\text{cop}_k[z]}\right)}. \qquad (11)$$

Notice that the denominator and the second term in the numerator above are constants, so the above equation is of the form $\ddot{x} = \beta \, (x - \alpha)$, which is linear and as such has an exact solution.

However, in the more general case, kinematic paths do not necessarily map to piecewise linear functions, but instead should be based on more sophisticated mappings. For instance, an efficient gait can be produced by following circular arcs, i.e. $p_{\text{com}[z]} = \left(r^2 - p_{\text{com}[x]}^2\right)^{0.5}$. In that case path accelerations for a given step can be expressed by differentiating the arc, i.e.

$$\begin{aligned} a_{\text{com}[z]} = &- \left(r^2 - p_{\text{com}[x]}^2\right)^{-1.5} p_{\text{com}[x]}^2 \, v_{\text{com}[x]}^2 \\ &- \left(r^2 - p_{\text{com}[x]}^2\right)^{-0.5} v_{\text{com}[x]}^2 \\ &- \left(r^2 - p_{\text{com}[x]}^2\right)^{-0.5} p_{\text{com}[x]} \, a_{\text{com}[x]} \end{aligned} \qquad (12)$$

where, r is the radius of the arc. Plugging the above acceleration dependency in (7) we get

$$a_{\mathrm{com}[x]} = \left(p_{\mathrm{com}[x]} - p_{\mathrm{cop}[kx]}\right) \frac{N\left(p_{\mathrm{com}[x]}, v_{\mathrm{com}[x]}, p_{\mathrm{cop}[kx]}\right)}{D\left(p_{\mathrm{com}[x]}, p_{\mathrm{cop}_k[x]}, p_{\mathrm{cop}_k[z]}\right)}, \qquad (13)$$

with

$$N \triangleq g - \left(r^2 - p_{\mathrm{com}[x]}^2\right)^{-1.5} p_{\mathrm{com}[x]}^2 v_{\mathrm{com}[x]}^2 - $$
$$\left(r^2 - p_{\mathrm{com}[x]}^2\right)^{-0.5} v_{\mathrm{com}[x]}^2 \quad (14)$$

$$D \triangleq \left(r^2 - p_{\mathrm{com}[x]}^2\right)^{0.5} - p_{\mathrm{cop}_k[z]} + $$
$$\left(p_{\mathrm{com}[x]} - p_{\mathrm{cop}_k[x]}\right)\left(r^2 - p_{\mathrm{com}[x]}^2\right)^{-0.5} p_{\mathrm{com}[x]}. \quad (15)$$

The acceleration of Eq. (13) is non-linear and therefore there is no closed-form solution anymore.

If the CoM geometric paths are generated by a more sophisticated planner with more complex kinematic dependencies, the acceleration profile will be non-linear with general expression

$$a_{\mathrm{com}[x]} = \left(p_{\mathrm{com}[x]} - p_{\mathrm{cop}[kx]}\right) \cdot \Phi\left(p_{\mathrm{com}[x]}, v_{\mathrm{com}[x]}, p_{\mathrm{cop}_k[x]}, p_{\mathrm{cop}_k[z]}\right), \qquad (16)$$

where, $\Phi(\cdot, \cdot, \cdot, \cdot)$ is a non-linear function, and as such does not have a closed-form solution.


3.3 State-space behavior prediction from perturbation theory

Our objective is to extract state-space trajectories for arbitrary kinematic CoM paths, $\mathbb{P}_k$. We refer to numerical integration to address the difficulty of solving non-linear differential equations such as Eq. (16). In particular, perturbation theory, has been widely used to solve the trajectory of celestial bodies and complex physical phenomena. Perturbation theory, is a set of methods that enable to approximate solutions from problems that do not have exact solutions, by looking into the solution of an exact related problem. In our case, we have the exact solution of accelerations given positions and contact points and we seek to approximate the solution of the CoM trajectory versus its velocity, i.e. the state-space trajectory.

Let us study our case. For simplicity, we call $x \triangleq p_{\mathrm{com}[x]}$ and therefore we can write Eq. (16) as

$$\ddot{x} = f(x, \dot{x}), \qquad (17)$$
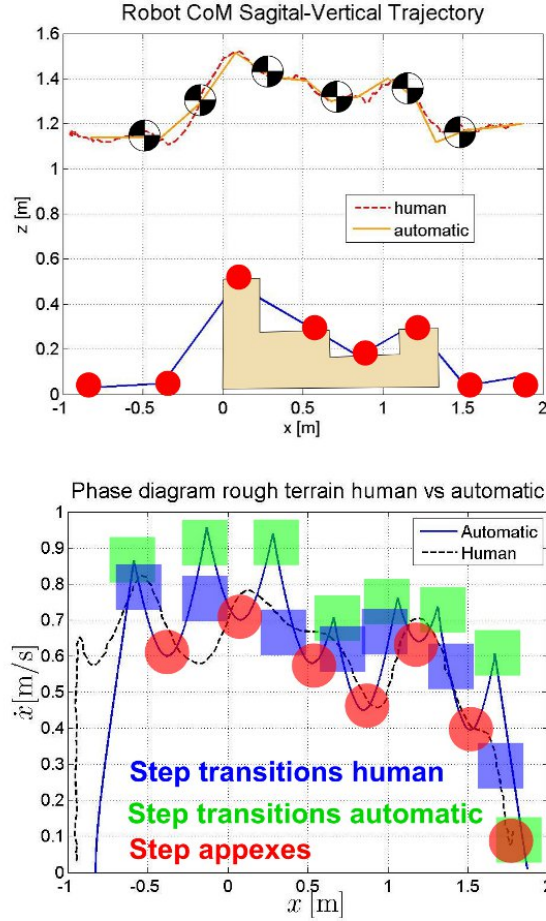
Fig. 3 Concatenation of steps: The top graph shows the kinematic trajectory of the human CoM (derived using motion capture) versus a piecewise linear approximation that we use to generate the automatic walking simulation. The red dots correspond to the position of the foot contacts. The bottom figure shows Matlab plots of Sagittal phase curves for the human and the automatic simulation. The red circles correspond to apexes of the steps. The green squares correspond to contact transitions of the automatic walk. The purple squares correspond to contact transitions of the human walk. Notice, that during the climbing of the first step of the stairs results in a smooth CoM pattern for the human walk. This is due to the smoothening effect of dual contact during the stance phase. This is not the case during the automatic walk because we have neglected the dual contact phase and therefore the transitions between contacts are instantaneous. Besides this difference, the rest of the walk correlates well.

where $f(x, \dot{x})$ is the RHS of Eq. (16). We assume that $\ddot{x}$ is approximately constant for small perturbations of x. By integrating over a small time period, ϵ (the perturbation), and for boundary conditions $(x_k, \dot{x}_k)$ we approximate the behavior of neighboring points as

$$\dot{x}_{k+1} \approx \dot{x}_k + \ddot{x}_k \epsilon, \tag{18}$$

$$x_{k+1} \approx x_k + \dot{x}_k \epsilon + 0.5 \, \ddot{x}_k \epsilon^2. \tag{19}$$

From Eq. (18) we find an expression of the perturbation in terms of the velocities and acceleration, $\epsilon \approx (\dot{x}_{k+1} - \dot{x}_k)/\ddot{x}_k$, and substituting in Eq. (19), with $\ddot{x}_k = f(x_k)$, we get

$$x_{k+1} \approx \frac{\left(\dot{x}_{k+1}^2 - \dot{x}_k^2\right)}{2 \, f(x_k)} + x_k, \tag{20}$$

which is the state-space approximate solution that we were looking for.

The pipeline for finding state-space trajectories goes as follows: (1) choose a very small time perturbations ϵ, (2) given known velocities $\dot{x}_k$ and accelerations $\ddot{x}_k$, and using Eq. (18), we get the next velocity $\dot{x}_{k+1}$, (3) using Eq. (20) we get the next position x_{k+1}, (4) plot the points $(x_{k+1}, \dot{x}_{k+1})$ in the phase-plane. We also notice, that we can iterate this recursion both forward and backward. If we iterate backward, we need to choose a negative perturbation ϵ.

Let us apply this method to the case of complex CoM paths as characterized by the general acceleration of Eq. (16). We apply it to two different trajectories, one where the CoM follows a downward linear path Fig. 2(a-c) and another one where the CoM follows a sinusoidal wave Fig. 2(d-f). The results of these two studies are shown in Fig. 2. In both cases the contact foot is located at point $\left(p_{\mathrm{cop}[x]}, p_{\mathrm{cop}[z]}\right) = (0,0)[m]$. For both studies, we provide various initial conditions at the apex (i.e. when the CoM is on top of the contact point), corresponding to the initial position and velocity, and using the proposed perturbation method obtain the phase diagram using forward and backward propagation. The reason why the Sagittal phase diagram of the linear CoM path is symmetrical is because Sagittal CoM accelerations are independent of vertical variations. This is not the case when the path is sinusoidal.

4 Motion Planning

Equipped with the perturbation method, which has allowed us to predict phase diagrams given arbitrary CoM paths and contact locations, we are now in the position to use it to plan dynamic walk in a very rough terrain.
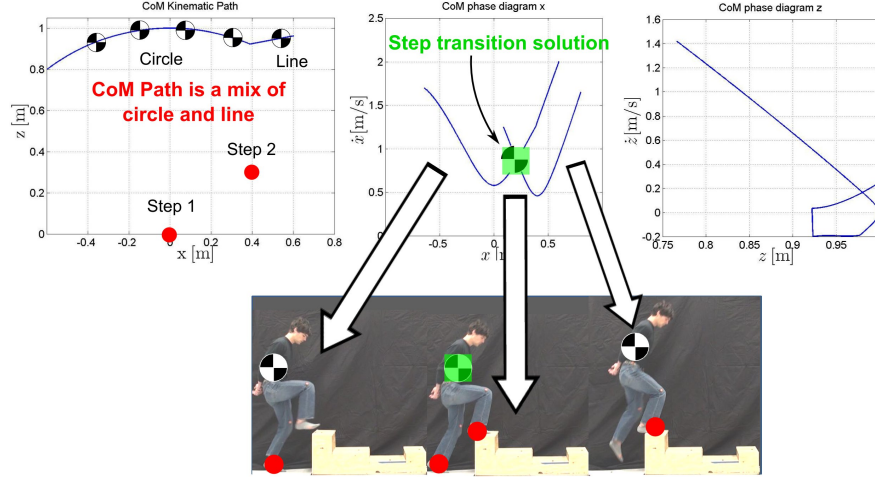
Fig. 4 Step solver: The center graph depicts phase curves for the two steps given the CoM path shown on the left. We fit polynomials and find the differential root between the adjacent curves to find the point of intersection.

4.1 Cascading multiple CoM phases

We have built a rough terrain set-up (see Fig. 4) in the Human Centered Robotics Lab at UT which consists of several steps of a variety of heights and widths. Figure 3, shows the resulting data of dynamically walking over this terrain, for both our human subject and the automatic planner presented throughout this paper. As we will see in the results section, the automatic planner approximates feet locations and CoM kinematics from the human, and automatically derives the dynamic walk. In particular, the CoM path has been approximated with piecewise linear segments, which are shown laid over the human CoM path extracted from a motion capture process.

Traversing the terrain of Fig. 4 involves making several steps, 7 in our example which are marked with red circles in Fig. 4. We are interested in displaying the phase diagram of the CoM for all steps for both the human and automatic walks. By plotting phase behavior for each step we can determine the intersections between neighboring steps (before and after), and therefore, derive the precise phase points to switch between steps. Because we have derived phase behavior for arbitrary CoM kinematics and feet locations, finding step intersections yields the motion and contact plan needed to dynamically walk over the rough terrain.

Let us focus on the automatic walk of the results section. We have used the perturbation method of Eq. (20) to derive phase curves for every step in forward and backward modes with respect to the contact point. Boundary conditions corresponding to CoM position and velocity are provided at the apex of each step. For this example we have used similar values than the

human. However, mimicking the human is not needed in the general case. We do it here to compare results between the planner and the human. The valleys of the bottom graph of Fig. 3 correspond to the deceleration/acceleration pattern of single steps. They are in fact the same type of curves than those predicted in Fig. 2, this time derived for every step of the desired sequence given the desired boundary conditions. As such, the green squares shown in Fig. 3 correspond to the points where two curves from neighboring steps have the same position and velocity and therefore correspond to the necessary contact transitions to switch to the next step.

The pipeline for automatically planning the walk in the rough terrain is therefore as follows: (1) develop CoM geometric path to overcome the terrain, (2) choose boundary conditions, i.e. position and velocity, of the CoM at the apex of each step, (3) using the perturbation method of Eq. (20), predict phase curves for each step, (4) find the phase intersections between neighboring steps which represent the phase point where the transition between steps need to occur, (5) the resulting multi-step phase diagram is the locomotion plan that will be fed to a control stage.

4.2 Phase Intersections to determine step transitions

From Fig. 3, it becomes clear that we derive the locomotion curves by finding the phase intersection between steps. We illustrate this procedure by studying the step to step transition on a particular example. Let us focus on the graphs shown in Fig. 4. The left graph shows our test example, with a CoM path consisting of a circular path first, continued by a line path. The motivation to use different curves is to illustrate the versatility of our method on working with any CoM path. The positions of the first and second step are also shown as red circles. The center graph depicts the phase curves for the first and second steps. We have used boundary conditions equal to $(x_0, \dot{x}_0) = (0, 0.6)$ and $(x_1, \dot{x}_1) = (0.4, 0.45)$ at the apexes of steps 1 and 2 respectively. The pictures showing the human are only to illustrate the switching strategy between steps but they have not been used to derive CoM geometric paths for this particular example.

Because the perturbation method of Eq. (20) is numerical, it is not obvious to derive the intersection point between CoM phases. Our approach goes as follows, (1) fit a polynomial of order 5 using Matlab's `polyfit()` function, to each of the two CoM phases, (2) subtract the two polynomials and find its roots using Matlab's `roots()` function, (3) discard imaginary roots, (4) get the point of intersection within CoM position range, and (5) extract the CoM velocity intersection by evaluating the polynomial at the CoM position intersection. If we apply this pipeline to the example of Fig. 4 we get that the step intersection is at $(x_s, \dot{x}_s) = (0.3, 0.7)$.

5 Results

Based on the methods described in the previous sections, we have conducted a study of locomotion in the Sagittal/vertical plane on a very rough terrain. Using a human-size robot model, we consider a variable stepped terrain with height variations between 0-40 [cm] and width variations between 20-40 [cm]. The goal of the planner is to maneuver the robot throughout the total length of the terrain. The speed specifications are determined to cruise the terrain at an average speed of 0.6 [m/s], although this choice could be arbitrary. We also assume that the robot starts and finishes with zero velocities and it increases velocity according to a trapezoidal profile similar to that of our human subject. Once more, our planner does not need human specifications, but we use them for comparison (see Fig. 3). Velocity specifications are given only at each new step, corresponding to the moment when the center of mass Sagittal position crosses the corresponding supporting foot, namely the apex of the step. We consider *steps* to be spanned from apex to apex. Also for simplicity, we consider only single-support phases, with instantaneous transition between feet. The contact locations and CoM geometrical path are given by the human subject and we assume a point mass model of the robot, with all of the weight located at its waist. The human subject traversing the terrain is shown in Fig. 6. His height is 184 [cm] and his weight is 80.5 [Kg] at the time of the experiment.

An analysis of the experiments is shown in the caption text of Figures 5 and 6.

6 Conclusions and outlook

Locomotion in very rough terrain can be formulated as a non-linear dynamical process. As such, it does not have a closed-form solution in most cases. We have resorted to perturbation theory as an effective tool to predict state space curves of CoM behavior. By cascading multiple phase curves of CoM behavior around step contacts and finding intersection points, we have generalized the planning of locomotion curves for arbitrary terrains. These prediction and planning methods represent important contributions to locomotion.

The strong correlation of locomotion curves shown in Figure 3, which compare artificial and human walks, demonstrate the validity of our methods. However, to be deployable, our method needs to further include multicontact stages such as when the two feet are in contact with the ground for some period of time. In such case, we will need to derive new dynamic models involving the effect of multicontact. We anticipate, that in such cases the effect of internal forces will play an important role of the acceleration profile. The Multicontact/Grasp matrix of [23] presents a powerful method to derive dynamic behavior given frictional constraints and tension forces between feet.
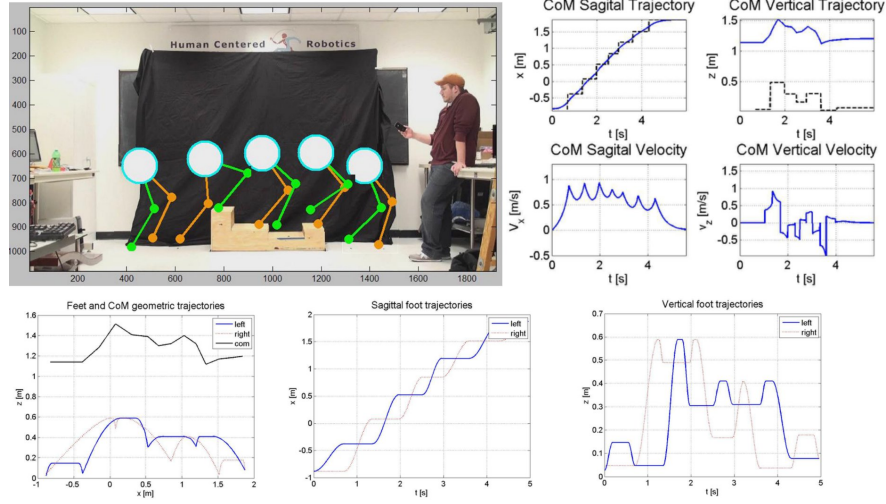
Fig. 5 Automatic locomotion planner: Using the proposed locomotion planner and based on human kinematic data, we create artificial CoM trajectories and determine contact transitions to achieve the desired design specifications of the walk. The snapshots on the upper left show a mix reality sequence derive from our planner. Time trajectories of CoM Sagittal and vertical behavior are shown to the right and are derived from the phase curves. A separate planner computes feet trajectories to synchronize with CoM behavior and switch step at the desired contact intersections.
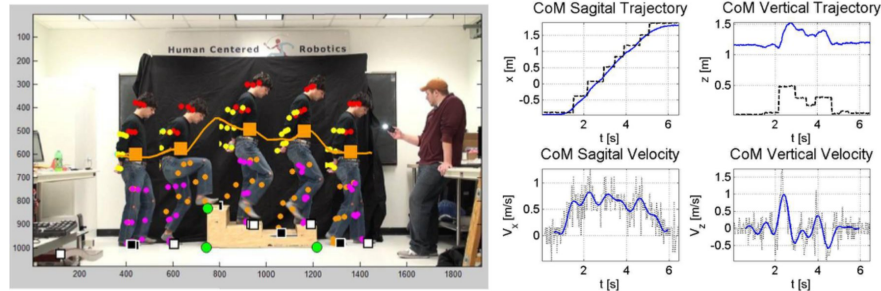
Fig. 6 Data extraction from human walk: A human subject walks over a rough terrain. Marker tracking is implemented and used to extract approximate CoM paths as well as Sagittal and vertical CoM trajectories and velocities.

Moreover, during multicontact phases, there will be multiple phase curves that will fulfill frictional constraints. This fact will enable to consider solutions that minimize some criterion such as effort.

Constraining the locomotion paths to the Sagittal-vertical plane has allowed us to tackle rough terrain locomotion effectively. However, practical locomotion needs to include the 3 dimensions of space. In such case, CoM geometric paths need to be planned in the full 3D space and a lateral dynamic

model similar to Equation (7) needs to be consider. Although this work has explore modeling and planning issues, an important component for locomotion is the choice of a controller. Operating in state space opens opportunities to implement robust controllers. We plan to tackle this problem in the context of whole-body compliant control [23]. The proposed methods can be used to tackle a wide variety of issues such as rough terrain locomotion, disturbance robustness, parameter uncertainty, internal force behavior, optimization of performance parameters, and feasibility conditions for planners.

References

1. K. Harada, S. Kajita, K. Kaneko, and H. Hirukawa, "Zmp analysis for arm/leg coordination," in *Proceedings of the IEEE/RSJ International Conference on Intelligent Robots and Systems*, Las Vegas, USA, October 2003, pp. 75–81.
2. S. Kajita, M. Morisawa, K. Harada, K. Kaneko, F. Kanehiro, K. Fujiwara, and H. Hirukawa, "Biped walking pattern generator allowing auxiliary zmp control," in *Intelligent Robots and Systems, 2006 IEEE/RSJ International Conference on*, october 2006, pp. 2993–2999.
3. M. Raibert, *Legged Robots that Balance*. MIT Press, Cambridge, Ma., 1986.
4. T. Bretl and S. Lall, "Testing static equilibrium for legged robots," *IEEE Transactions on Robotics*, vol. 24, no. 4, pp. 794–807, August 2008.
5. C. Collette, A. Micaelli, C. Andriot, and P. Lemerle, "Robust balance optimization control of humanoid robots with multiple non coplanar grasps and frictional contacts," in *Proceedings of the IEEE International Conference on Robotics and Automation*, Pasadena, USA, May 2008.
6. J. Pratt and R. Tedrake, "Velocity-based stability margins for fast bipedal walking," in *Fast Motions in Biomechanics and Robotics*, M. Diehl and K. Mombaur, Eds., 2006, vol. 340, pp. 299–324.
7. T. McGeer, "Passive dynamic walking," *The International Journal of Robotics Research*, vol. 9, no. 2, pp. 62–68, 1990.
8. A. Goswami, B. Espiau, and A. Kermane, "Limit cycles and their stability in a passive bipedal gait," in *Proceedings of the IEEE International Conference on Robotics and Automation*, April 1996, pp. 246–251.
9. K. Mombaur, H. Bock, J. Schloder, and R. Longman, "Self-stabilizing somersaults," *Robotics, IEEE Transactions on*, vol. 21, no. 6, pp. 1148 – 1157, december 2005.
10. A. Ruina, J. Bertram, and M. Srinivasan, "A collisional model of the energetic cost of support work qualitatively explains leg sequencing in walking and galloping, pseudoelastic leg behavior in running and the walk-to-run transition," *Journal of Theoretical Biology*, no. 237, pp. 170–192, 2005.
11. T. Takuma and K. Hosoda, "Controlling the walking period of a pneumatic muscle walker," *The International Journal of Robotics Research*, vol. 25, no. 9, pp. 861–866, 2006.
12. E. Westervelt, J. Grizzle, C. Chevallereau, J. Choi, and B. Morris, *Feebdack control of dynamic bipedal robt locomotion*. CRC Oress, 2007.
13. B. Stephens and C. Atkeson, "Modeling and control of periodic humanoid balance using the linear biped model," in *Humanoid Robots, 2009. Humanoids 2009. 9th IEEE-RAS International Conference on*, december 2009, pp. 379 –384.
14. J. Rummel, Y. Blum, and A. Seyfarth, "Robust and efficient walking with spring-like legs," *Bioinspiration & Biomimetics*, vol. 5, no. 4, p. 046004, 2010.

15. M. Wisse, A. Schwab, R. van der Linde, and F. van der Helm, "How to keep from falling forward: elementary swing leg action for passive dynamic walkers," *Robotics, IEEE Transactions on*, vol. 21, no. 3, pp. 393 – 401, june 2005.
16. K. Byl and R. Tedrake, "Metastable walking machines," *The International Journal of Robotics Research*, vol. 28, no. 8, pp. 1040–1064, 2009.
17. I. R. Manchester, U. Mettin, F. Iida, and R. Tedrake, "Stable dynamic walking over uneven terrain," *The International Journal of Robotics Research*, vol. 30, no. 3, pp. 265–279, 2011.
18. M. Spong, J. Holm, and D. Lee, "Passivity-based control of bipedal locomotion," *Robotics Automation Magazine, IEEE*, vol. 14, no. 2, pp. 30 –40, june 2007.
19. M. Zucker, J. Bagnell, C. Atkeson, and J. Kuffner, "An optimization approach to rough terrain locomotion," in *Robotics and Automation (ICRA), 2010 IEEE International Conference on*, may 2010, pp. 3589 –3595.
20. K. Hauser, T. Bretl, K. Harada, and J. Latombe, "Using motion primitives in probabilistic sample-based planning for humanoid robots," in *Workshop on Algorithmic Foundations of Robotic (WAFR)*, New York, USA, July 2006.
21. K. Bouyarmane and A. Kheddar, "Multi-contact stances planning for multiple agents," in *Proceedings of the IEEE International Conference on Robotics and Automation*, Shanghai, May 2011.
22. L. Sentis and B. Fernandez, "Com state space cascading manifolds for planning dynamic locomotion in very rough terrain," in *Proceedings of Dynamic Walking 2011*, Jena, Germany, July 2011.
23. L. Sentis, J. Park, and O. Khatib, "Compliant control of multi-contact and center of mass behaviors in humanoid robots," *IEEE Transactions on Robotics*, vol. 26, no. 3, pp. 483–501, June 2010.